Alternative Fe–O_2 Bond Lengths in O_2 Adducts of Iron Porphyrins: Implications for Hemoglobin Cooperativity

Geoffrey L. Woolery,[†] Mark A. Walters,[†] Kenneth S. Suslick,*[‡] Linda S. Powers,*[§] and Thomas G. Spiro*[†]

Contribution from the Department of Chemistry, Princeton University, Princeton, New Jersey 08540, Department of Chemistry, University of Illinois, Urbana, Illinois 61801, and AT&T Bell Laboratories, Murray Hill, New Jersey 07974. *Received May 9, 1984*

Abstract: The extended fine structure (EXAFS) of the Fe K edge X-ray absorption spectrum has been analyzed for O_2 adducts of "picket-fence" iron(II) porphyrin complexes with hindered bases: $Fe(O_2)(TpivPP)(2\text{-MeIm})\cdot C_2H_5OH$ and $Fe(O_2)(TpivPP)(1,2\text{-Me}_2Im)$ (TpivPP = 5,10,15,20-($\alpha,\alpha,\alpha,\alpha$)-(*o*-pivaloylamidophenyl)porphyrinate, 2-MeIm = 2-methylimidazole, 1,2-Me_2Im = 1,2-dimethylimidazole). The first shell peaks of the Fourier transforms were filtered and backtransformed, and analyzed for the distances from the Fe to the coordinated atoms (one O, one imidazole N, and four pyrrole N). For the 2-MeIm complex at −150 °C, the Fe–O distance was 1.90 Å, in agreement with X-ray crystallography. For the 1,2-Me_2Im complex, however, the Fe–O distance was 1.77 Å, the same as the crystallographically determined distance for the O_2 adduct with the unhindered base, 1-MeIm (1-methylimidazole). *These results establish that two Fe–O distances are available to O_2 adducts with hindered bases*: one with a shorter Fe–O bond and a consequently longer Fe–N_{Im} bond, and the second vice versa. These two structures offer a plausible explantation for the cooperativity in O_2 binding previously observed for the solid (ethanol-free) adducts of these complexes; the low- and high-affinity binding regions may be due to the formation of the long and short Fe–O bonded structures successively. A similar structure change may take place within the T state of hemoglobin for which there exists substantial evidence of restraint on the proximal imidazole; initial ligand binding may occur via a long Fe–O bond, which could be followed by rearrangement to a short Fe–O bonded structure.

The synthesis and study of synthetic analogues to O_2 binding heme proteins continue to give fresh insights into the molecular structure and function of such systems.[1] Steric protection provided by porphyrin substituents has proved an especially useful approach since it dramatically enhances the kinetic stability of iron–dioxygen complexes by preventing the bimolecular pathway leading to irreversible autoxidation.[1c,2,3] The dioxygen adducts of "picket-fence" metalloporphyrins (Figure 1) have been effectively utilized as models for structural, functional, and physical properties of oxymyoglobin and oxyhemoglobin.[1c,2]

The steric bulk of certain axial ligands (e.g., 2-methylimidazole and 1,2-dimethylimidazole), when complexes to the iron(II) "picket-fence" porphyrin, hinder the approach of the Fe atom into the plane of the porphyrin and provide models of the lowered O_2 affinity, and the T-state of hemoglobin.[2i] The remarkable observation of *cooperative* O_2 binding[2l,o] to crystalline samples of[4] Fe(TpivPP)(2-MeIm) and Fe(TpivPP)(1,2-Me_2Im) (Figure 2) has led us to explore a variety of physical and structural probes of these complexes and their O_2 adducts. The X-ray diffraction crystal structures demonstrated an appreciably lengthened Fe–O bond (1.90 Å vs. 1.77 Å) for the hindered imidazole complex,[2g,o] $Fe(O_2)(TpivPP)(2\text{-MeIm})\cdot C_2H_5OH$, compared to the unhindered $Fe(O)_2(TpivPP)(1\text{-MeIm})$,[2a,b,h] thus providing a direct connection between bond length and O_2 affinity. Surprisingly, the Fe–O_2 stretching frequency found in resonance Raman (RR) spectra[2n,5] of $Fe(O_2)(TpivPP)(2\text{-MeIm})$ or $Fe(O_2)(TpivPP)(1,2\text{-Me}_2Im)$ were only a few cm^{-1} below that of $Fe(O_2)(TpivPP)(1\text{-MeIm})$, rather than the 100-$cm^{-1}$ decrease predicted by Badger's rule.[6] Furthermore, the solid state O_2 binding was found to show cooperativity only for desolvated Fe(TpivPP)(2-MeIm) and Fe(TpivPP)(1,2-Me_2Im), but *not* for $Fe(TpivPP)(2MeIm)\cdot C_2H_5OH$, for which the structures had been determined.[2o] We have now determined, via EXAFS analysis, that these complexes show a dramatic variation in the Fe–O_2 and Fe–N_{Im} distances which offers a plausible explanation for their cooperative O_2 binding and which may have application to the mechanism of Hb cooperativity.

Experimental Section

The synthesis and characterization of these complexes have been detailed elsewhere.[2g,k,l,n,o] EXAFS data collection was conducted at the Stanford Synchrotron Radiation Laboratory during dedicated operation of the SPEAR storage ring (40–80 mA, 3.0 GeV), using beam line II-3. The methods used for sampling and detection and data analysis are

[†] Princeton University.
[‡] University of Illinois.
[§] Bell Laboratories.

(1) (a) Jones, R. D.; Summerville, D. A.; Basolo, F. *Chem. Rev.* **1979**, *79*, 139. (b) Perutz, M. F. *Annu. Rev. Biochem.* **1979**, *48* 327. (c) Collman, J. P.; Halbert, T. R.; Suslick, K. S. In "Metal Ion activation of Dioxygen"; Spiro, T. G., Ed.; Wiley: New York, 1980; pp 1–72. (d) Traylor, T. G. *Acc. Chem. Res.* **1981**, *14*, 102. (e) Jameson, G. B.; Ibers, J. A. *Comments Inorg. Chem.* **1983**, *2*, 97.

(2) (a) Collman, J. P.; Gagne, R. R.; Reed, C. A.; Robinson, W. T.; Rodley, G. A. *Proc. Natl. Acad. Sci. USA* **1974**, *71*, 1326. (b) Collman, J. P.; Gagne, R. r.; Reed, C. A.; Halbert, T. R.; Lang, G.; Robinson, W. T. *J. Am. Chem. Soc.* **1975**, *97*, 1427. (c) Collman, J. P.; Brauman, J. I.; Suslick, K. S. *J. Am. Chem. Soc.* **1975**, *97*, 7185. (d) Spartalian, K.; Lang, G.; Collman, J. P.; Gagne, R. R.; Reed, C. A. *J. Chem. Phys.* **1975**, *63*, 5375. (e) Collman, J. P.; Brauman, J. I.; Halbert, T. R.; Suslick, K. S. *Proc. Natl. Acad. Sci. U.S.A* **1976**, *73*, 333.. Collman, J. P.; Brauman, J. I.; Doxsee, K. M.; Halbert, T. R.; Hayes, S. E.; Suslick, K. S. *J. Am. Chem. Soc.* **1978**, *100*, 2761. (g) Jameson, G. B.; Molinaro, S. S.; Ibers, J. A.; Collman, J. P.; Brauman, J. I.; Rose, E.; Suslick, K. S. *J. Am. Chem. Soc.* **1978**, *100*, 6769. (h) Jameson, G. B.; Rodley, G. A.; Robinson, W. T.; Gagne, R. R.; Reed, C. A.; Collman, J. P. *Inorg. Chem.* **1978**, *17*, 850. (i) Collman, J. P.; Brauman, J. I.; Doxsee, K. M.; Halbert, T. F.; Suslick, K. S. *Proc. Natl. Acad. Sci. U.S.A* **1978**, *75*, 564. (j) Burke, J. M.; Kincaid, J. R.; Peters, S.; Gagne, R. R.; Collman, J. P.; Spiro, T. G. *J. Am. Chem. Soc.* **1978**, *100*, 6083. (k) Collman, J. P.; Brauman, J. I.; Doxsee, K. M.; Halbert, T. R.; Suslick, K. S. *Proc. Natl. Acad. Sci. U.S.A.* **1978**, *75*, 564. (l) Collman, J. P.; Brauman, J. I.; Rose, E.; Suslick, K. S. *Proc. Natl. Acad. Sci. U.S.A.* **1978**, *75*, 1052. (m) Collman, J. P.; Brauman, J. I.; Doxsee, K. M. *Proc. Natl. Acad. Sci. U.S.A.* **1979**, *76*, 6035. (n) Walters, M. A.; Spiro, T. G.; Suslick, K. S.; Collman, J. P. *J. Am. Chem. Soc.* **1980**, *102*, 6857. (o) Jameson, G. B.; Molinaro, F. S.; Ibers, J. A.; Collman, J. P.; Brauman, J. I.; Rose, E.; Suslick, K. S. *J. Am. Chem. Soc.* **1980**, *102*, 3224.

(3) (a) Linard, J. E.; Ellis, P. E., Jr.; Budge, J. R.; Jones, R. D.; Basolo, F. *J. Am. Chem. Soc.* **1980**, *102*, 1869. (b) Budge, J. R.; Ellis, P. E., Jr.; Jones, R. D.; Linard, J. E.; Basolo, F.; Baldwin, J. E.; Dyer, R. L. *J. Am. Chem. Soc.* **1979**, *101*, 4760. (c) Hashimoto, T.; Dyer, R. L.; Crossley, M. J.; Baldwin, J. E.; Basolo, F. *J. Am. Chem. Soc.* **1982**, *104*, 2101. (d) Ward, B.; Wang, C. B.; Chang, C. K. *J. Am. Chem. Soc.* **1981**, *103*, 5236. (e) Suslick, K. S.; Fox, M. M. *J. Am. Chem. Soc.* **1983**, *105*, 3507. (f) Suslick, K. S.; Fox, M. M.; Reinert, T. J. *J. Am. Chem. Soc.* **1984**, *106*, 4522.

(4) Abbreviations: Hb, hemoglobin; Im, imidazole; 2-MeIm, 2-methylimidazole; 1,2-Me_2Im, 1,2-dimethylimidazole; $P_{1/2}$, partial pressure of gas at half-saturation; TpivPP, $\alpha,\alpha,\alpha,\alpha$-5,10,15,20-tetrakis[*o*-pivalamidophenyl]-porphyrinate(2−), the "picket-fence" porphyrin; TPP, 5,10,15,20-tetraphenylporphyrinate(2−); RR, resonance Raman; N_p, pyrrolic nitrogen atoms of the porphyrin; N_{Im}, the coordinated nitrogen atom of the axial imidazole; EXAFS, extended X-ray absorption fine structure.

(5) (a) Hori, H.; Kitagawa, T. *J. Am. Chem. Soc.* **1980**, *102*, 3608. (b) Kerr, E. A.; Mackin, H. C.; Yu, N.-T. *Biochemistry*, in press.

(6) Herschbach, D. R.; Laurie, V. W. *J. Chem. Phys.* **1961**, *35*, 458.

0002-7863/85/1507-2370$01.50/0

Table I. Fe–Ligand Bond Lengths(Å) in O_2 Adducts

	Fe–O	$Fe–N_{Im}$[a]	Fe–O[b] + $Fe–N_{Im}$	$Fe–N_P$[c]	method[d]
(O_2)FeTpivPP(1-MeIm)	1.75 (2)[e]	2.07 (2)	3.82	1.98 (2)	xstal[f]
				1.98 (1)	EXAFS[g]
(O_2)FeTpivPP(2-MeIm)·EtOH	1.898 (7)	2.107 (4)	4.005	1.998 (4)	xstal[h]
	1.90 (3)	2.07 (4)	3.97	1.99 (3)	EXAFS[f]
(O_2)FeTpivPP(1,2-Me_2Im)	1.77 (3)	2.29. (4)	4.06	1.99 (3)	EXAFS[f]
oxyMb	1.83 (6)	2.07 (6)	3.90	1.95 (6)	xstal[j]
	1.80 (2)	2.06 (2)	3.86	2.02 (2)	EXAFS[k]
oxyHb, α chains, R State	1.67 (8)	1.95 (10)	3.62	1.98 (4)	xstal[l]
oxyHb, β chains, R State	1.83 (13)	2.06 (9)	3.89	1.96 (9)	xstal[l]
oxyNg, α chains, T State	1.8 (1)	2.3 (2)	4.1		xstal[m]

[a] Fe–N(imidazole) bond length. [b] Sum of Fe–O and $Fe–N_{Im}$ bond lengths. [c] Fe–N(pyrrole) bond length. [d] X-ray crystallographic (xtal) of EXAFS determination. [e] Standard deviation (xtal) or estimated uncertainty (EXAFS) in the last digit. [f] Reference 2a,b,h at 297 K. [g] Reference 7f at 300 K. [h] Reference 20 at 294 K. [i] This work at 123 K. [j] Reference 19a at 261 K. [k] Reference 7e at 4 K. [l] Reference 19b at 271 K. [m] Reference 19c.

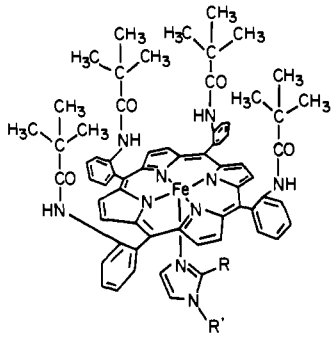

Figure 1. The "picket-fence" porphyrin complexes. R = H, R′ = CH_3: Fe(TpivPP)(1-MeIm). R = CH_3, R′ = H: Fe(TpivPP)(2-MeIm). R = CH_3, R′ = CH_3: Fe(TpivPP)(1,2-Me_2Im).

described elsewhere.[7a] At least four scans were averaged to enhance signal/noise. Figure 3 shows the background-subtracted, k^3-weighted EXAFS modulation for the 1,2-Me_2Im and 2-MeIm complexes, at −150 °C. The scattering amplitude is significantly lower (see the ordinate scale in Figure 3) for $Fe(O_2)$(TpivPP)(1,2-Me_2Im) than for $Fe(O_2)$-(TpivPP)(2-MeIm)·EtOH at −150 °C, because of interference among the scattering contributions from the distinctly inequivalent bonds (Fe–O and Fe–N) of the former (Table I).

These data were Fourier transformed, and the first-shell Fourier peak was filtered, backtransformed, and fit to model compounds [FeTPP$(Im)_2$ for Fe–N (1.99 Å) and Fe(acetylacetonate)$_3$ for Fe–O (1.99 Å)], using the procedures described previously.[7a,b] These involve fitting the filtered data of a given scattering shell with two sets of scattering atoms, using four parameters for each set: N, r, $\Delta\sigma$, and ΔE_0, which are the number of scatterers, the average scattering distance, and the changes in Debye–Waller factor and edge energy, relative to the model compounds. N and $\Delta\sigma^2$ are generally highly correlated and ΔE_0 is small (<3 eV) and slightly correlated to r.[7a,b] For the present complexes, the Fe first shells have three sets of unresolved scatterers: one O atom, one imidazole-N atom, and four pyrrole-N atoms. Possible solutions for each contribution were mapped by the residuals squared using a two-scatterer nonlinear least-squares fitting procedure[7a,b,e] with amplitude ratios fixed[7c–e] at 4/2 (to isolate the $Fe–N_{pyr}$ scattering) or at 5/1 (to isolate the Fe–O or $Fe–N_{Im}$ scattering). Only one physically reasonable solution was found for each contribution. These three distances were then tested for consistency[7e] with a calculation using all three sets of scatterers, with r and N held constant for each set of scatterers. This highly constrained test allows only variation of the parameters that are correlated with those held fixed and hence has fewer variables than the two-scatterer fits. The sum of the residuals squared was smaller by at least a factor of 2 than the

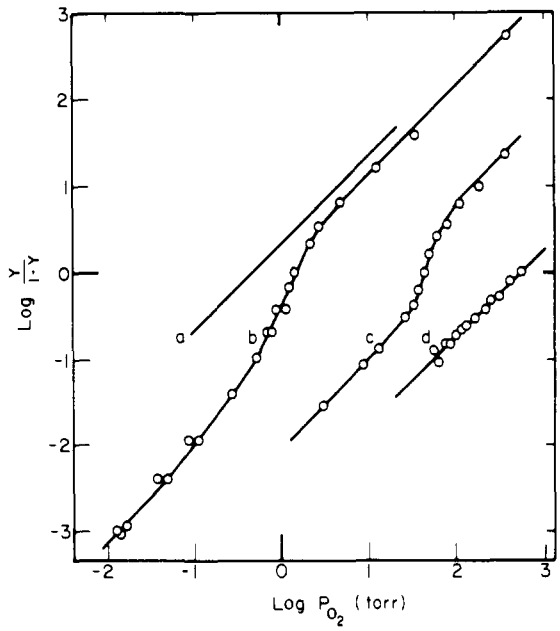

Figure 2. Cooperative O_2 Binding to Fe(TpivPP)(B). (a) B = 1-MeIm. (b) B = 2-MeIm. (c) B = 1,2-Me_2Im. (d) B = 2-MeIm-C_2H_5OH. Taken from ref 2b.

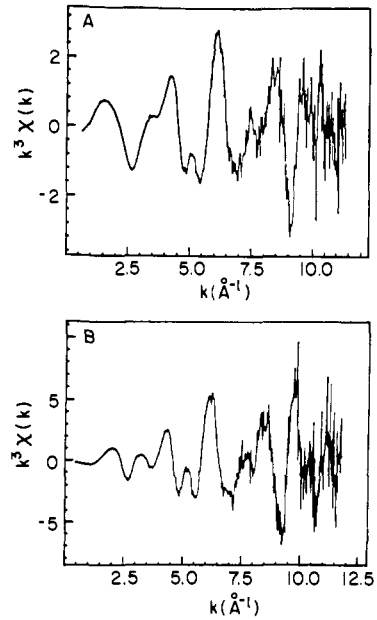

Figure 3. Background-subtracted, k^3-weighted EXAFS modulations of (a) $Fe(O_2)$(TpivPP)(1,2-Me_2Im), at −150 °C, and (b) $Fe(O_2)$-(TpivPP)(2-MeIm)·EtOH at −150 °C.

(7) (a) Powers, L. S.; Chance, B.; Ching, Y.; Angiolillo, P. *Biophys. J.* **1981**, *34*, 465. (b) Lee, P. A.; Citrin, P.; Eisenberger, P. M.; Kincaid, B. M. *Rev. Mod. Phys.* **1981**, *53*, 769. (c) Peisach, J.; Powers, L.; Blumberg, W. E.; Chance, B. *Biophys. J.* **1982**, *38*, 277. (d) Chance, B.; Fischetti, R.; Powers. L. S. *Biochemistry* **1983**, *22*, 3820. (e) Powers, L.; Sessler, J. L.; Woolery, G. L.; Chance, B. *Biochemistry*, in press. (f) Eisenberger, P.; Shulman, R. G.; Kincaid, B. M.; Brown, G. S.; Ogawa, S. *Nature (London)* **1978**, *274*, 30. (g) At 25 °C, the EXAFS of $Fe(O_2)$(TpivPP)(2-MeIm)·C_2H_2OH appeared to be a superposition of contributions from structures with long and short $Fe–O_2$ bonds, suggesting that the long-bonded structure is stabilized by ethanol molecules in the lattice, which are slowly lost during irradiation at 25 °C. Conversion to the short-bonded structure upon loss of ethanol provides a natural explanation for the failure to observe a significantly lower $Fe–O_2$ stretching frequency in the RR spectrum.[2n] Even though precautions had been taken to maintain a low temperature (−70 °C), it is likely that local heating by the laser beam was sufficient to drive ethanol off.

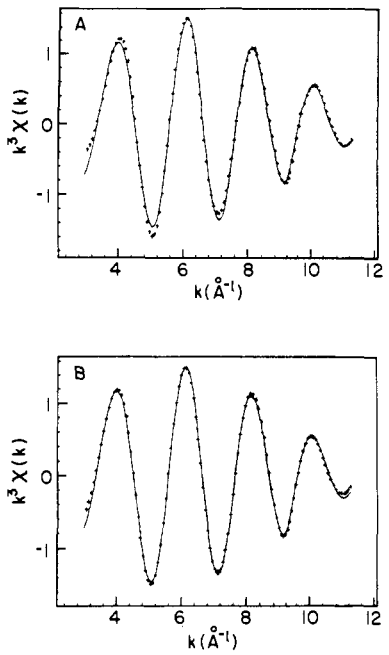

Figure 4. First-shell Fourier-filtered data of (O_2)FeTpivPP(1,2-Me_2Im) normalized to one iron atom (–) vs. (a) two-scatterer fit (+) with fixed amplitude ratio of 5 N atoms (4 Fe–N_p and 1 Fe–N_{Im}) to 1 O atom (1 Fe–O). (b) Constrained consistency test (+) using data given in Table I.

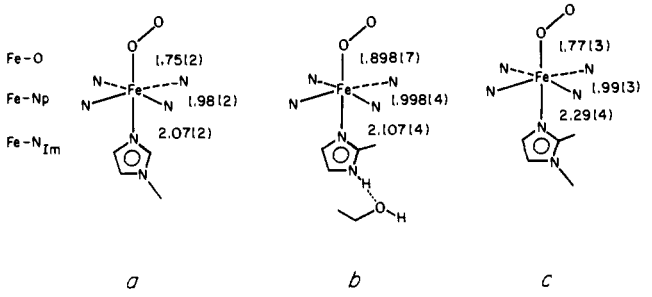

Figure 5. Structural parameters of picket-fence iron porphyrin dioxygen complexes: (a) $Fe(O_2)$(TpivPP)(1-MeIm); X-ray crystal structure. (b) $Fe(O_2)$(TpivPP)(2-MeIm)·C_2H_5OH; X-ray crystal structure and EXAFS. (c) $Fe(O_2)$(TpivPP)(1,2-Me_2Im); EXAFS.

lowest value obtained in any of the two-scatterer fits. A comparison of the best fit of the filtered data to the two-scatterer model and to the three-scatterer consistency test is given in Figure 4. To assure that these three distances together constituted a true minimum, each distance was then allowed to vary one at a time. The best-fit distances remained within 0.03 Å of the initial estimates (obtained from the two-scatterer fits). In order to determine the error in each of these contributions, a single distance was changed, but not allowed to vary, until the sum of the residuals squared ($\sum^2$) increased by a factor of 2. These are given in the parentheses of Table I and accurately represent the ± uncertainty. A detailed discussion of the constrained two-scatterer procedure and the three-scatterer consistency test together with comparison of the results of this method and those obtained from crystallography for several heme proteins and models is given by Powers et al.[7e]

Results and Discussion

The structural parameters determined from the EXAFS spectra are presented in Table I and shown schematically in Figure 5. The variation in Fe–O distances are particularly striking. The Fe–O distance is only 1.77 Å for $Fe(O_2)$TpivPP(1,2-Me_2Im), which is essentially identical with that of the unhindered Fe-(O_2)(TpivPP)(1-Me-Im), whereas a long distance of 1.90 Å is observed for $Fe(O_2)$(TpivPP)(2-MeIm)·C_2H_5OH (in agreement with the crystallographic determination at 21 °C).[7g]

For comparison and illustration, Table II presents the fitting results from the three-atom type consistency test for data on

Table II.[a] Three-Atom Type Consistency Tests for $Fe(O_2)$(TpivPP)(1,2-Me_2Im)

model	bond	$\bar{r}$	N	$\Delta\sigma^2$	ΔE_0	$\sum^2$
	Fe–N_P	1.99	4	-6.1×10^{-3}	5.3	0.22
A	Fe–N_{Im}	2.29	1	-8.1×10^{-3}	8.8	
	Fe–O	1.77	1	-9.1×10^{-3}	−1.9	
	Fe–N_P	1.99	4	-3.4×10^{-3}	4.9	0.27
B	Fe–N_{Im}	2.07	1	-6.2×10^{-3}	**26.7**	
	Fe–O	1.90	1	-7.6×10^{-3}	−7.7	
	Fe–N_P	1.99	4	-8.4×10^{-3}	3.9	0.54
C	Fe–N_{Im}	2.29	1	-5.5×10^{-3}	10.0	
	Fe–O	1.90	1	$\mathbf{-3.8 \times 10^{-2}}$	−6.1	
	Fe–N_P	1.99	4	-5.4×10^{-3}	2.7	0.38
D	Fe–N_{Im}	2.07	1	$\mathbf{-3.5 \times 10^{-2}}$	14.2	
	Fe–O	1.77	1	-1.2×10^{-2}	−2.8	
	Fe–N_P	1.99	4	-4.2×10^{-3}	0.5	0.31
E	Fe–N_{Im}	2.07	1	-1.8×10^{-3}	**24.3**	
	Fe–O	2.07	1	$\mathbf{-4.0 \times 10^{-2}}$	5.4	
	Fe–N_P	1.99	4	-6.1×10^{-3}	−2.0	0.19
F	Fe–N_{Im}	1.77	1	-6.2×10^{-3}	**−22.1**	
	Fe–O	1.77	1	$\mathbf{-6.1 \times 10^{-2}}$	**−53.8**	
	Fe–N_P	1.99	4	-8.0×10^{-3}	2.5	0.78
G	Fe–N_{Im}	2.29	1	$\mathbf{-3.1 \times 10^{-2}}$	−12.1	
	Fe–O	2.29	1	-1.0×10^{-2}	10.4	

[a] $\bar{r}$ = bond distance (Å); N = number of atoms; $\Delta\sigma^2$ = calculated Debye–Waller factor (Å^2); ΔE_0 = change in edge energy (eV); $\sum^2$ = sum of residuals squared for each structural model. Boldfaced values are physically unreasonable, as discussed in the text.

$Fe(O_2)$(TpivPP)(1,2-Me_2Im), given a variety of structural models. Model A is the best solution and was determined by the methods described in the Experimental Section. The others were chosen simply to represent forced solutions to alternative structural models: for example, when a single bond distance is made short (i.e., $\bar{r}$(Fe–N_{Im}) = 2.07) or long (i.e., $\bar{r}$(Fe–O) = 1.90 Å); these are not found as solutions in the two-atom type fitting procedure. Model B uses the geometry of $Fe(O_2)$(TpivPP)(2-MeIm)·C_2H_5OH, with a short Fe–N_{Im} bond and a long Fe–O bond. Model C uses a geometry with a long Fe–N_{Im} and a long Fe–O bond, etc. In every case except for the optimal fit of Model A, one or more of the fitting parameters are physically unreasonable, and are indicated by boldfacing in Table II. For example, $\Delta\sigma^2 \sim -1 \times 10^{-2}$ Å^2 for a solution at room temperature; values which are several times this are unreasonable for a chemically bonded ligand and mathematically indicate that the fitting program is trying to decrease the amplitude of this contribution since N is fixed. Similarly, $\Delta E_0 \sim \pm 7$ eV for all compounds which have the same absorbing atoms (as expected from theoretical calculations); larger values indicate that the distance held fixed is not compatible with the others. Solutions which produce $\sum^2$ values that differ by a factor of 2 are considered significant. Thus, only Model A shown in Table II (and listed in Table I) is physically reasonable. These data prove that we can easily distinguish, for example, between a lengthened Fe–O distance and a lengthened Fe–N_{Im} distance.

The EXAFS results establish that the steric restraint to O_2 binding imposed by hindered imidazoles can be accommodated in alternative ways. Comparison of the crystal structures of $Fe(O_2)$(TpivPP)(1-MeIm)[2a,b,h] and $Fe(O_2)$(TpivPP)(2-MeIm)·C_2H_5OH[2g,o] reveals that the lengthened Fe–O distance of the latter is chiefly due *to a switch in the position of the Fe atom relative to the porphyrin plane*. The position of the iron atom changes from 0.03 Å toward the O_2 ligand in $Fe(O_2)$(TpivPP)(1-MeIm) to 0.08 Å toward the imidazole ligand in $Fe(O_2)$(TpivPP)(2-MeIm)·C_2H_5OH, while the Fe–N_{Im} is lengthened by only 0.04 Å. The nonbonded distances between O_2 and the pyrrole-N atoms are nearly the same for the two structures. In simultaneously accommodating the steric requirements of O_2 and the hindered base present in $Fe(O_2)$(TpivPP)(2-MeIm)·C_2H_5OH, the Fe atom retains a near-normal bond to the imidazole, at the expense of

a lengthened Fe–O_2 bond. A plausible alternative would have been a normal Fe–O_2 bond and a lengthened bond to the base. This is indeed the situation for the 1,2-Me_2Im adduct for which the EXAFS analysis gave a long Fe–N_{Im} bond, 2.29 Å, and a short Fe–O_2 bond (see Table I). The sum of the Fe–O_2 and Fe–N_{Im} distances are nearly the same for the 2-MeIm and 1,2-Me_2Im adducts, as expected for these two alternative solutions to the steric restraint problem.

What determines the energy balance between these alternative structures? In (O_2)FeTpivPP(2-MeIm)·C_2H_5OH, the ethanol molecule is H-bonded to the N3 proton of the 2-MeIm ligand. It has been argued that the H-bond increases the donor strength of the imidazole, increasing its interaction with Fe.[8] In addition, the H-bond anchors the 2-MeIm in a particular orientation, which may favor a short Fe–N_{Im} bond. We speculate that a preferred orientation may provide for the remarkable observation of cooperativity in O_2 binding to solid samples of the ethanol-free 2-MeIm adduct, or of the 1,2-MeIm adduct.[2l] Their O_2 binding curves are characterized by low- and high-affinity regions, at low and high O_2 saturations, with a cooperative transition in between,[2l,o] as shown in Figure 2. We suggest that the low-affinity region is associated with the initial formation of a structure with a long Fe–O_2 bond, determined by the imidazole orientation in the deoxy lattice, and that the high-affinity region is associated with the subsequent switch to the short-bonded structure, established by EXAFS. Cooperativity would then be associated with the required phase change to a new lattice accommodating the imidazole orientation required by the short Fe–O_2 bonded structure. When this reorientation is blocked, as in the ethanol solvate, only the long Fe–O_2 bonded structure is accessible, and noncooperative, low-affinity O_2 binding is observed.[2l,o] In solution the two structures are expected to be freely interconvertible; consistent with this, FeTpivPP(1,2-MeIm) in toluene solution shows noncooperative binding with an affinity close to the geometric mean of the low- and high-affinity values in the solid state.[2l] The high value of the Fe–O_2 stretching frequency[2n] in solutions of Fe(O_2)(TpivPP)(2-MeIm) establishes the structure with the short Fe–O_2 bond as the more stable equilibrium form, in the absence of the additional constraints of the deoxy crystal lattice.

Are these structures relevant to the problem of hemoglobin (Hb) cooperativity? It is significant that in (T state) deoxyHb there is a protein imposed tilting of the proximal imidazole relative to the heme normal.[9] The resulting nonbonded contact with one of the pyrrole-N atoms[10] may be responsible[11] for the lowered stretching frequency of the deoxyHb Fe–N_{Im} bond in the T state relative to the R state, as observed by RR spectroscopy.[12,13] Thus, the hindered-base heme complexes appear to be quite apt models of T-state Hb, the steric hindrance mimicking the nonbonded repulsion induced by the tilted proximal imidazole. By analogy with these models, it is possible that O_2 binding to Hb also proceeds via an initially long Fe–O_2 bonded adduct. Relaxation to a short-bonded structure might be connected with the T → R quaternary change, or it might precede this change, depending on how tightly the proximal imidazole orientation is linked to the protein structure.

The published evidence favors a short Fe–O_2 bonded structure for the ligated T state.[16,17] First, the Fe–O_2 stretching RR band is at a normal frequency, 570 cm^{-1}, for O_2 adducts of the mutant Hb's Milwaukee or Kansas,[16] and is shifted by less than 3 cm^{-1} upon addition of IHP (inositol hexaphosphate) which is believed to induce a switch to the T state. Likewise, $\nu_{Fe\text{-}CO}$ in the CO adduct of Hb Kansas is uninfluenced by the quaternary structure,[17] as is $\nu_{Fe\text{-}F}$ in the fluoride complex of met-Hb.[18] Most interestingly, a very recent X-ray crystallographic analysis[19c] of partially oxygenated Hb, in which the O_2 is bound to the α but not to the β chain hemes in an essentially T quaternary structure, appears to show short Fe–O_2 bonds (1.8 (1) Å) but *lengthened* Fe–N_{Im} bonds (2.23–2.50 Å vs. 1.94–2.06 Å in R state HbO_2). These bond lengths are consistent with our EXAFS-derived distances for (O_2)FeTpivPP(1,2-Me_2Im) (Table I). These results suggest that in half-ligated Hb, the imposed restraint on the coordinated, proximal imidazole may weaken the Fe–N_{Im} bond, rather than the Fe–O_2 bond.

Acknowledgment. This work was supported in part by NIH Grants HL 12526 (to T.G.S.) and HL 25934 and an R.C.D.A. (to K.S.S.), by American Heart Association Grant 83923 (to K.S.S.), and by a Sloan Research Fellowship (to K.S.S.). Synchrotron radiation time was provided by the Stanford Synchrotron Radiation Laboratory, supported by NSF Grant DMR 77-27489, in cooperation with the Stanford Linear Accelerator and the U.S. Department of Energy. Helpful discussion and criticism by Professor J. P. Collman, Stanford University, are gratefully appreciated.

Registry No. Fe(O_2)(TpivPP)(2-MeIm), 95340-79-7; Fe(O_2)(TpivPP)(1,2-Me_2Im), 92419-61-9; Fe(O_2)(TpivPP)(1-MeIm), 75559-87-4; Fe(TpivPP)(1-MeIm), 52215-89-1; Fe(TpivPP)(2-MeIm), 75598-80-0; Fe(TpivPP)(1,2-Me_2Im), 75597-81-8; O_2, 7782-44-7.

(8) (a) Stein, P.; Mitchell, M.; Spiro, T. G. *J. Am. Chem. Soc.* **1980**, *102*, 7795. (b) Walker, F. A.; Lo, M.-W.; Ree, M. T. *J. Am. Chem. Soc.* **1976**, *98*, 5552. (c) Nappa, M.; Valentine, J. S.; Snyder, P. A. *J. Am. Chem. Soc.* **1977**, *99*, 5799.
(9) Baldwin, J. M; Chothea, C. *J. Mol. Biol.* **1979**, *129*, 175.
(10) Gelin, B. R.; Karplus, M. *Proc. Natl. Acad. Sci. U.S.A.* **1977**, *74*, 801.
(11) Friedman, J. M.; Rousseau, D. L.; Ondrias, M. R.; Stepnoski, R. A. **Science** (*Washington, D.C.*) **1982**, *218*, 1244.
(12) Nagai, K.; Kitagawa, T. *Proc. Natl. Acad. Sci. U.S.A.* **1980**, *77*, 2033.
(13) Weakened H-bonding to the N_ϵ proton of the proximal imidazole had been suggested[8a] as an explanation of the Fe–Im frequency lowering, but this explanation now seems unlikely in the light of correlations of NMR chemical shifts of the N_ϵ protons[14] and of a porphyrin skeletal vibrational frequency, ν_4.[15]
(14) LaMar, G. N.; DeRopp, J. S. *J. Am. Chem. Soc.* **1982**, *104*, 5203.
(15) Ondrias, M. R.; Rousseau, D. L.; Shelnut, J. A.; Simon, S. R. *Biochemistry* **1982**, *21*, 3428.
(16) Nagai, K.; Kitagawa, T.; Morimoto, H. *J. Mol. Biol.* **1980**, *136*, 271.
(17) Tsubaki, M.; Srivastava, R. B.; Yu, N.-T. *Biochemistry* **1982**, *21*, 1132.
(18) Asher, S. A.; Schuster, T. M. *Biochemistry* **1981**, *20*, 1866.
(19) (a) Simon, S. E. V. *Nature* (*London*) **1978**, *273*, 247. (b) Shaanan, B. *Nature* (*London*) **1982**, *296*, 684. (c) Brzozowski, A.; Derewenda, Z.; Dodson, E.; Dodson, G.; Grabowski, M.; Liddington, R.; Skarzynski, T.; Vallely, D. *Nature* (*London*) **1984**, *307*, 74.